Comparative Study of the Mechanical Properties of Different Tungsten Materials for Fusion Applications

S Krimpalis[1], K Mergia[1,*], S Messoloras[1], A Dubinko[2,3], D Terentyev[2], K. Triantou[1], J Reiser[4] and G Pintsuk[5]

[1]*National Centre for Scientific Research „Demokritos", Institute of Nuclear and Radiological Science and Technology, Energy and Safety, 15310 Aghia Paraskevi, Athens, Greece*
[2]*SCK•CEN, Institute for Nuclear Material Sciences, 2400 Mol, Belgium*
[3]*Department of Applied Physics, Ghent University, 9000 Ghent, Belgium*
[4]*Karlsruhe Institute of Technology (KIT), Institute for Applied Materials,76344 Eggenstein-Leopoldshafen, Germany*
[5]*Forschungszentrum Jülich GmbH, EURATOM Association, 52425 Jülich, Germany*

Abstract

The mechanical properties of tungsten produced in different forms before and after neutron irradiation are of considerable interest for their application in fusion devices such as ITER. In this work the mechanical properties of two tungsten (W) products with different microstructures are investigated using depth sensing nanoindentation and transmission electron microscopy. A neutron irradiation campaign of these materials is underway within the EUROfusion project in order to progress our basic understanding of neutron irradiation effects on W. The hardness and elastic modulus are determined as a function of the penetration depth, loading/unloading rate, holding time at maximum load and the final surface treatment. The results are correlated with the microstructure as investigated by SEM and TEM measurements.

[*] Corresponding author: K. Mergia, kmergia@ipta.demokritos.gr, tel. +30 2106503706

1. Introduction

Tungsten (W) is a candidate plasma facing material for fusion reactors due to its high melting point, high thermal conductivity and good sputtering resistance [1]. However, it suffers from brittle fracture at low temperatures and this causes a limitation of its exploitation. Several methods of microstructure modification [2, 3, 4, 5, 6] have been proposed to cope with the low ductility problem. Within the framework of the EUROfusion project WPMAT [7] a neutron irradiation campaign of tungsten materials is underway in order to advance the understanding of the basic phenomena underlying the neutron irradiation effects on tungsten and provide experimental validation of theoretical models. As a first step towards this goal it is crucial to obtain reference data of the non-irradiated materials.

Nowadays, nanoindentation is widely used for the study of the mechanical properties of materials on the nano-scale because of the ease, speed and sample simplicity with which it can be carried out [8]. Current technologies allow the accurate measurement of loads as low as 0.1 μN and displacements of about 0.1 nm. Several works report on the use of nanoindentation for determining the mechanical properties of tungsten [9,10,11,12,13,14].

The mechanical properties of the materials depend strongly on their microstructure and to this end two classes of W material are investigated, namely, cold-rolled tungsten in sheet form and tungsten in forged bar form. The rationale behind the selection of these materials lies on the fact that a) it has been shown that cold cold-rolling is a process which increases the ductility and strength of W at room temperature [15] and b) the forged bar material is one of the options of the plasma facing material for ITER and the best characterized tungsten grade in Europe in terms of mechanical, thermo-physical and high heat flux properties [16]. Differences in microstructure are expected to influence the mechanical properties of these materials. In the current study, by employing depth sensing nanoindentation, the values of hardness (H) and elastic modulus (E) of the two tungsten materials are determined and the influence of indentation depth, loading and unloading rates and holding time at the maximum load are discussed and correlated with the microstructure.

2. Materials and methods

Two types of tungsten (W) materials are investigated in the current study, namely low temperature rolling W sheet (details can be found Ref. [17]) and W forged bar, as described in Table 1. The W materials in sheet and bar form are both produced by PLANSEE SE in a powder metallurgical route consisting of sintering and rolling or forging. From these materials, disks with thickness of about 1 mm and diameter around 12 mm were sectioned which were subsequently mechanically polished using diamond suspension to obtain mirror quality surface. For the disks sectioned from the W forged bar, the direction perpendicular to the specimen front surface is along the bar axis. The final step of the surface treatment of the investigated materials for the measurement of the mechanical properties is presented in Table 1. For the "cold rolled" W sheet both electropolishing and chemomechanical polishing were employed in order to assess the effect of surface finishing on the nanoindentation results. According to the literature sufficiently long chemomechanical polishing with alkaline colloidal silica is able to remove the damaged layers caused by mechanical polishing using diamond paste [18].

Table 1. Material description

Material	Description	Surface treatment
„cold rolled" W sheet-A 1 mm thickness purity >99.97%	Heavily deformed low temperature rolling sheet (below 1200 ^{o}C) and stress relief annealing [17]	Chemomechanical polishing with colloidal silica containing 5% CrO_3 aqeous solution (20 g in 100 ml water)
„cold rolled" W sheet-B 1 mm thickness purity >99.97%	Heavily deformed low temperature rolling sheet (below 1200 ^{o}C) and stress relief annealing [17]	Electropolishing at 20 V in 4% aqueous solution of NaOH
W forged bar 36×36 mm^2 cross section purity >99.97%	Fabrication by forging/hammering from two orthogonal directions	Electropolishing at 20 V in 4% aqueous solution of NaOH

The mechanical properties, hardness (H) and Elastic modulus (E), were measured using depth sensing nanoindentation employing NANOVEA's mechanical tester. A Berkovich indenter and a maximum load of 400 mN were used. The calibration of the instrument was carried out

employing fused silica and its calibration was verified by performing measurements on a standard stainless steel sample. For each test condition a minimum of ten indents spaced by 200 μm were performed in order to get statistically meaningful data. The optical microscope was used to select indented area free from visible defects.

During an indentation experiment an indenter of specified geometry, in our case a Berkovich indenter, penetrates into the surface of the material under investigation with constant loading rate. When the load reaches its set maximum value the indenter is held at this maximum load for a time period (holding time), and then the unloading takes place usually at the same rate with the loading. The load and penetration depth are measured versus time and these measurements are combined to give a load versus depth curve. The unloading part of the curves are analyzed following the method developed by Oliver and Pharr [19, 20] to obtain H and E.

For the W electromechanically polished sheet, the hardness and elastic modulus were measured as a function of penetration depth for loading/unloading rate of 90 mN/min and holding time at maximum load of 100 s. Also on the same material the effect of loading/unloading rate and holding time at maximum load was investigated for the maximum load of 400 mN.

The specimens for TEM samples were mechanically polished from both sides using SiC paper to achieve 70-100 μm thickness and further cut with a wire cutter into pieces to fit 3 mm TEM grids. They were polished again from both sides with 4000 grit SiC paper to remove the remnants of a glue, rinsed in acetone and ethanol and then glued on 3 mm copper grids with an aperture of 1 mm. Finally, TEM specimens were polished electrochemically with a solution of 1.5 wt% NaOH in water with applied voltage of 30 V. The specimens were investigated with JEOL 2010 TEM operating at 200 kV and JEOL 3010 TEM operating at 300 kV. The TEM images were taken using bright condition to enhance resolution of dislocation lines in the same style as presented in Figs.2 and 3. The average dislocation density was measured following the methodology used in [21]. Each calculation requires a TEM micrograph, corresponding diffraction pattern and convergent beam electron diffraction (CBED) pattern. Several calculations at different areas of the specimen were performed to get an average number of dislocation density. In Digital Micrograph software, provided with the image sensor of a microscope, a circle is drawn randomly in an image and the number of intersections of it with dislocation lines is counted. Dislocation density is then calculated as $\rho = 2N/Lt$, where N is the

number of intersections of the circle with dislocation lines, L – length of the circle, t – local thickness of the specimen at the area of the image. The length of the circle is automatically calculated in the Digital Micrograph software. The local thickness of the specimen is determined from the CBED pattern and diffraction pattern.

3. Results and Discussion

3.1 Microstructure

Tungsten produced by rolling has a plate-like grain shape while forging results in a uniaxial elongated grain shape [16].

The microstructure of W sheet and W bar materials, as examined after being etched by scanning electron microscopy are presented in Fig.1 (S1 *supplementary file*). For the W sheet the grains are elongated along a certain direction which presumably is the rolling direction. The visible grain size is in the range 2-4 μm in the direction of the elongation and about 1-2 μm perpendicular to it. For the W bar the surface normal of the sample is along the bar axis, and the grain size perpendicular to this direction is around 2 μm. The holes present in the W bar are due to the mechanical grinding and polishing of the material. It is noted that for the indentation measurements electropolishing was performed for adequate long time to ensure the removal of the damaged layers.

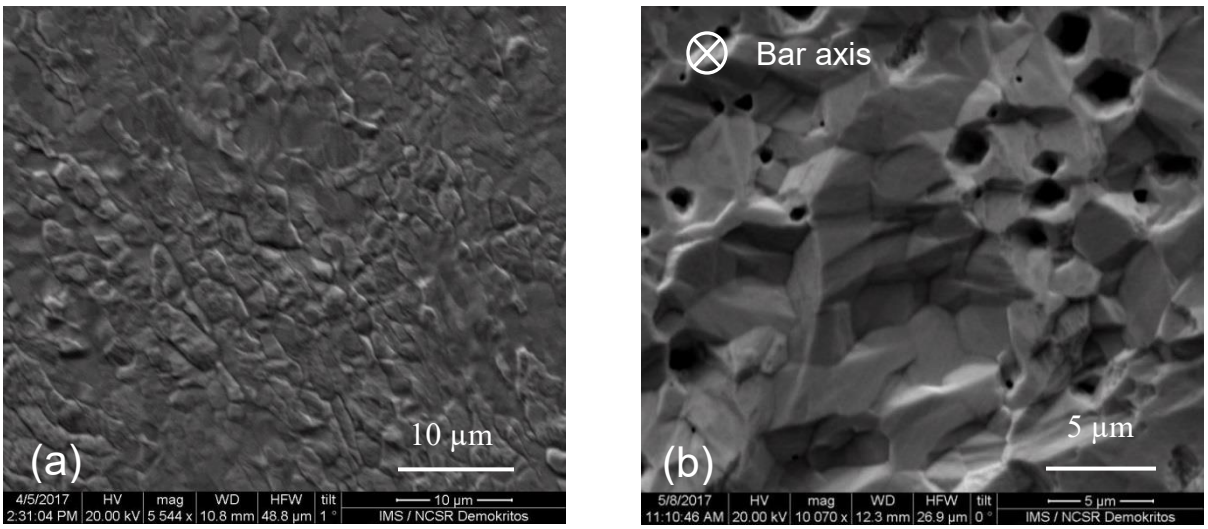

Fig.1. SEM image of the W microstructure in sheet (a) and forged bar (b) form.

The TEM images of the W sheet and bar are presented in Figs. 2 and 3, respectively. For the W sheet the visible grain size is in the range 1.5 – 2 μm, while it presents a dense tangled dislocation network (Fig.2b) with an average dislocation density of 3.25×10^{13} m^{-2} and low angle grain boundaries (Fig.2c). Regarding the W forged bar, due to the hammering of the bar from two orthogonal directions, the grains are needle-like and are elongated along the bar axis, as shown in Fig.3. TEM measurements show that sub-grains are also elongated and their size varies in the range 0.6 – 1.7 μm and 2.3 – 4 μm, normal to and along the elongation directions, respectively. The dislocation density is about $(4\text{-}8)\times10^{12}$ m^{-2}, depending on the particular sub-grain, and is being 4.5×10^{12} m^{-2} on average.

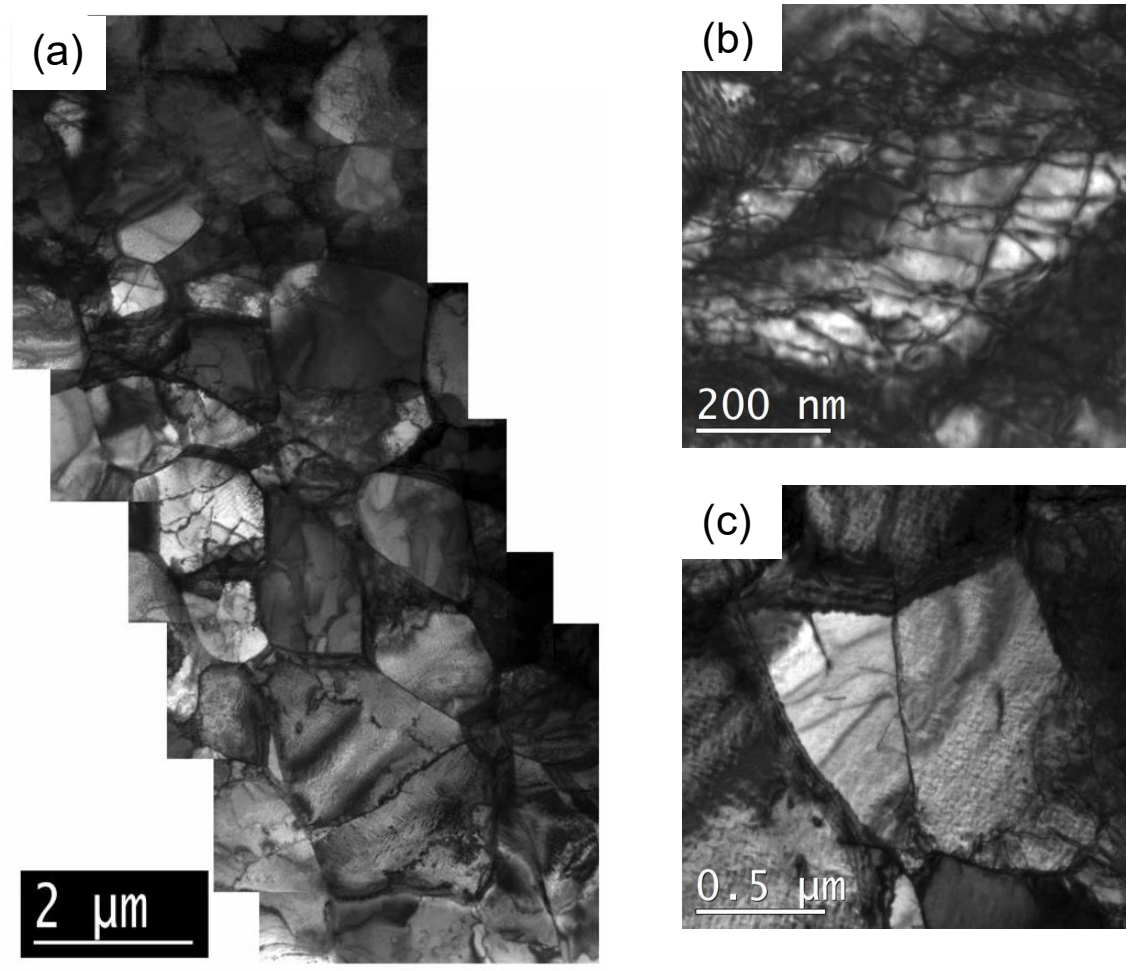

Fig.2. TEM images of the W sheet: (a) Bright field, (b) dislocation network and (c) low angle grain boundaries.

Fig.3. TEM image of the forged W bar.

3.2 Nanoindentation

The influence of the indentation depth on the obtained values of H and E was investigated for the chemomechanically polished W-sheet using different maximum loads, in the range 50 to 400 mN. The loading/unloading rate was kept at 90 mN/min and the holding time at maximum load at 100 s. Typical load – depth curves for three different maximum loads are presented in Fig.4 (S2 *supplementary file*). For the investigated W samples no pop-in behaviour [9] is observed at the beginning of the loading process (Fig. 4). It is noted that the imprint of the indent has as an edge size on each side varying between 3.3 and 12 μm for the maximum load of 50 and 400 mN, respectively, and for loads greater than 150 mN comprises several grains/sub-grains.

From the unloading part of the load-depth curves and assuming a power law for the load versus depth [19], the hardness and the elastic modulus were determined as a function of the penetration depth (Fig.5).

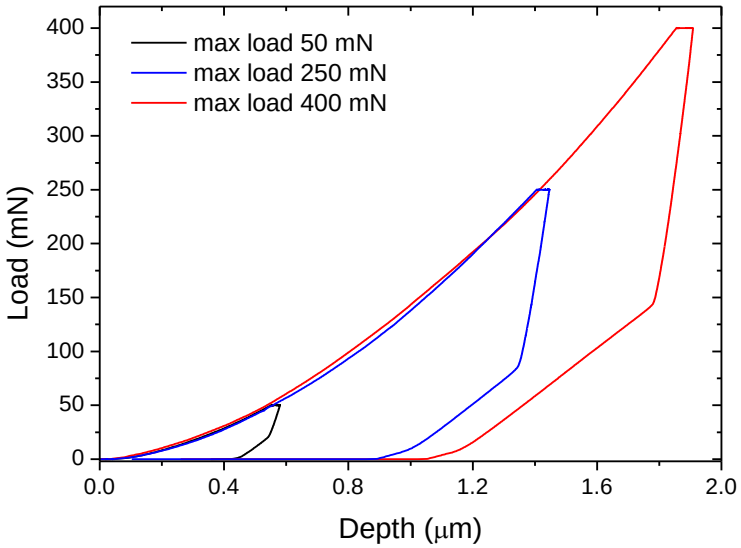

Fig. 4. Load-depth curves for W sheet-A for three different maximum loads with loading/unloading rate of 90 mN/min and holding time at maximum load 100 s.

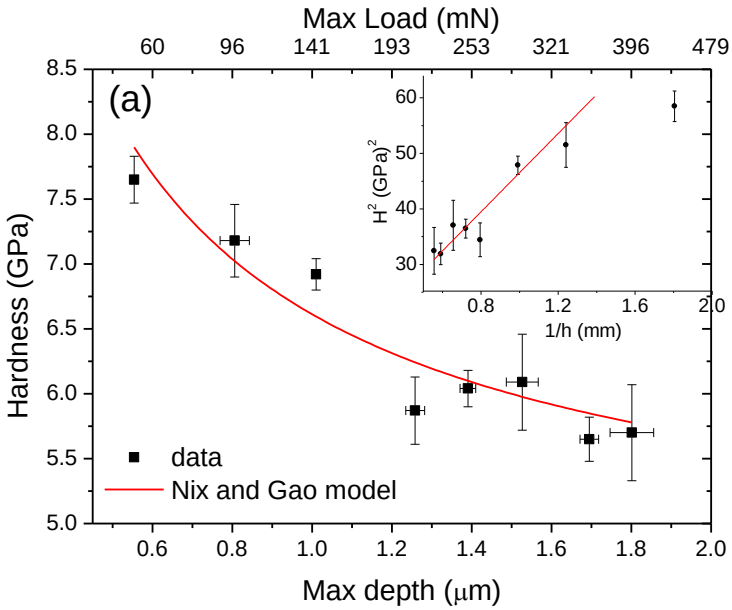

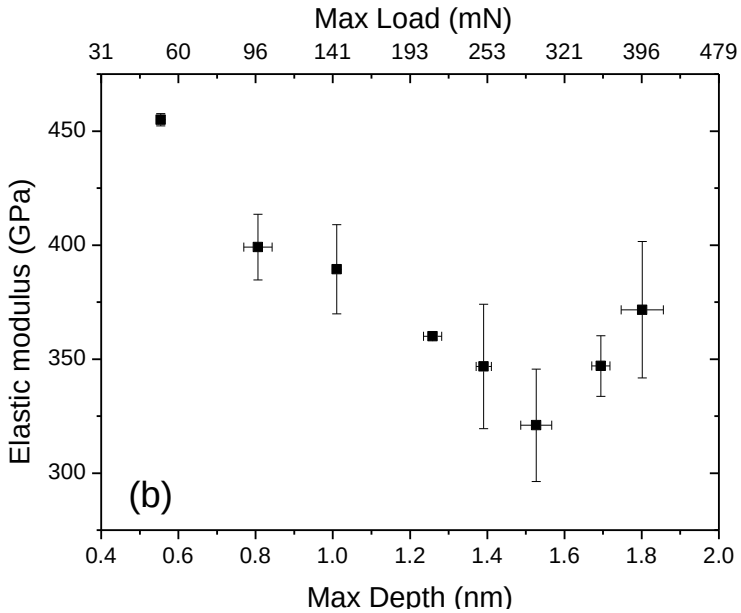

Fig. 5. Hardness (a) and elastic modulus (b) as a function of penetration depth for W sheet-A.

It is observed that the hardness decreases as the penetration depth increases and after 1.2 μm it remains almost constant within error bars with an average value of H_{av} =5.9 ± 0.2 GPa (Fig.5a). This behavior is understood by the well-known indentation size effect (ISE) [22], wherein the hardness is observed to increase with decreasing indentation size, especially in the sub-micrometer depth regime, and it is attributed to the evolution of geometrically necessary dislocations (GNDs) beneath the indenter, which gives rise to the strain gradients that cause enhanced hardening [23]. The derived value for H_{av} compares well with the average (in both directions, perpendicular and along the rolling direction) hardness of the "cold rolled" W sheet reported by Reiser et al. [24] and found to be 530 HV 0.1. The ISE effect has been found in previous studies of W material [25].

The application of the Nix-Gao formula ([22], solid line is Fig.5a)

$$\frac{H}{H_0} = \sqrt{1 + \frac{h^*}{h}} \tag{1}$$

where H is the hardness for a given depth, h, of indentation, H_0 is the hardness in the limit of infinite depth and h^* is a characteristic length that depends on the shape of the indenter , the shear modulus and H_0, gives $H_0 = 4.5 \pm 0.4\,\text{GPa}$ and $h^* = 1.13 \pm 0.38\,\mu\text{m}$. The plot of the square of hardness versus the inverse of the indentation depth, h, at each load, shown in the inset of Fig. 5a, reveals that a linear relation predicted by the Nix−Gao model agrees satisfactorily with the experimental results, within error bars, for depths larger than 0.8 μm.

The modified Nix-Gao model enables relating the characteristic length h^* with the dislocations statistically stored in the lattice (SSDs), ρ_s, as [22, 26, 27]

$$\rho_s = \frac{3}{2}\frac{1}{f^3}\frac{\tan^2\theta}{bh^*} \tag{2}$$

where θ the angle between the surface of the material and the surface of the indenter, b the Burgers vector of the dislocations and f a correction factor for the size of the plastic zone [26]. In the present work $\tan\theta$=0.358, f = 1.9 [26], and b = 0.286 nm. The application of Eq. (2) gives a dislocation density of 8.7 × 10^{13} m^{-2}. This value is in reasonable agreement with the dislocation density determined by TEM measurements, taking into account the error bar associated with TEM measurements.

The H_0 value agrees well with the Vickers hardness (440 HV) determined for this material by Wirtz et al. [16].

The elastic modulus as a function of penetration depth (Fig.5b) shows a continuous decrease from 452 GPa at 0.5 μm depth to about 320 GPa at 1.5 μm depth and subsequently it slightly increases to 370 GPa for the maximum penetration depth of 1.8 μm. The increase of the elastic modulus for depths larger than about 1.5 μm could be attributed to the interaction between the Plastically Affected Zone (PAZ) boundary and the grain/subgrain boundary. One may infer that at indentation depths around 1.5 μm the interaction between the PDZ boundary and the grain/sub-grain boundary becomes dominating in the process of the indentation, which leads to the hindering of dislocation propagation and causes dislocation pile-up formation [25]. It is noted that for indentation depths larger than 1.5 μm, slight dislocation pile-up is observed around the imprint of the indents (see Fig. 6, supplementary file S3).

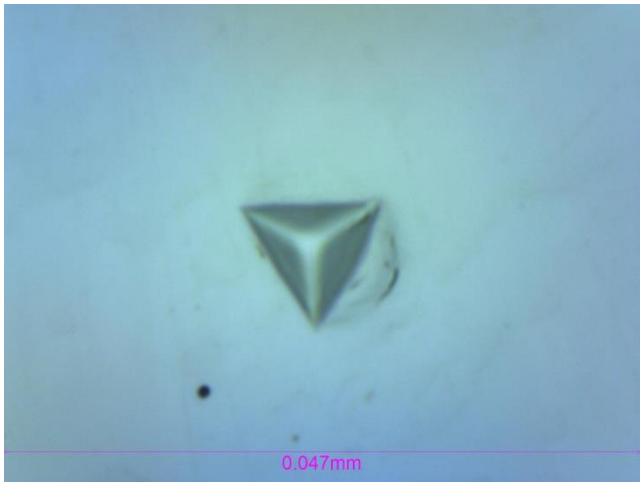

Fig. 6. The imprint of the indent at 250 mN maximum load showing material pile-up effect.

Furthermore, in order to assess the effect of the loading/unloading rate and the holding time at maximum load on hardness and elastic modulus, indentation tests were performed for various values of these parameters at the maximum load of 400 mN which corresponds to an indentation depth of about 1.8 μm. In Fig. 7 the hardness and elastic modulus variation versus holding time at the maximum load of 400 mN and for loading/unloading rate of 90 mN/min are depicted. The shaded area represents the 10% standard deviation of the average value (solid line in Fig.7) of all the measurements. No significant variation is observed for the hardness and the elastic modulus, or in other words, the variation of the obtained values from their average is within 10%. The average values for H and E are 5.64±0.08 GPa and 338±27 GPa, respectively.

Regarding the loading rate effect on hardness and elastic modulus, only for the hardness a systematic slight increase in observed (Fig.8), which must be associated with the strain hardening effect. The average value of the elastic modulus is 345±21 GPa which is in agreement with the average value obtained for the different holding times at maximum load (Fig.7).

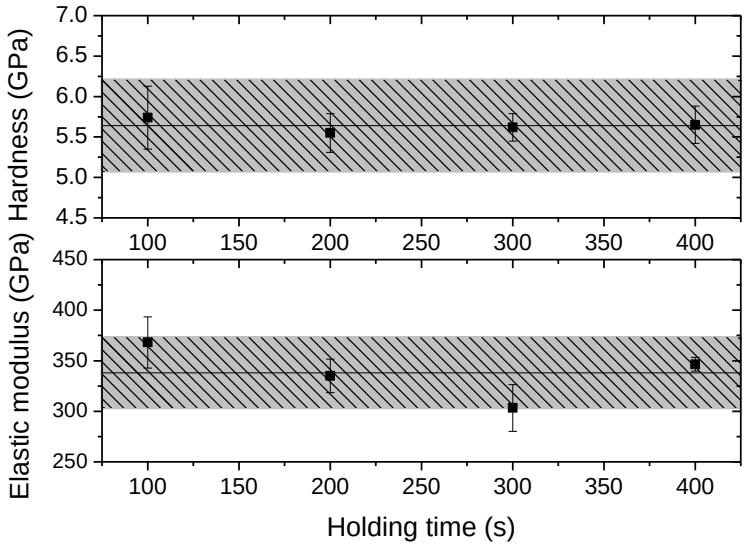

Fig.7. Hardness and elastic modulus versus holding time at the maximum load of 400 mN and for loading/unloading rate of 90 mN/min for W sheet-A.

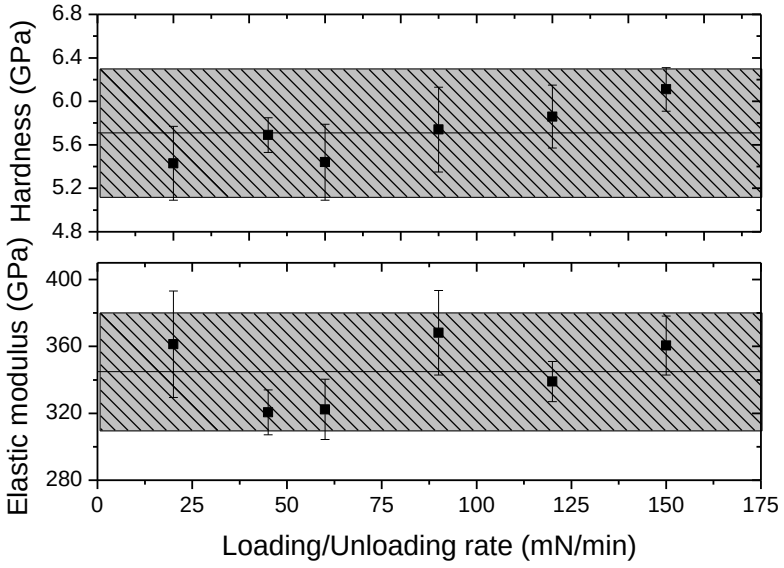

Fig.8. Hardness and elastic modulus versus loading/unloading rate for 400 mN maximum load and holding time 100 s for W sheet-A.

Having shown above that there is no significant dependence of the hardness and elastic modulus on the loading/unloading rate and the holding time at the maximum load, the load-depth curves for the W materials under investigation were measured for 400 mN maximum load and for

holding time and loading/unloading rate of 100 s and 90 nm/min, respectively. It is noted that the penetration depth for 400 mN maximum load is around 1.8 μm and any surface effects are expected to be negligible.

The obtained values of hardness and elastic modulus for all the investigated materials at the maximum load of 400 mN are presented in Fig.9. Both electropolished and chemomechanically polished samples from the W sheet have the same hardness, indicating that the quality of the surface is equivalent for both. However, the hardness for the W bar is around 15% lower. The higher hardness value of W sheet compared to W bar correlates with the higher dislocation density found by TEM in W sheet. Regarding the elastic modulus there is a considerable difference, outside the range of the statistical error bar, between W sheet chemomechanically polished and electropolished (Fig.9). Since the results of Fig.9 correspond to a penetration length of 1.8 μm, this difference is not expected to be due to the different surface treatment but it is attributed to the enhanced grinding of the electropolished W sheet from 1 mm to 0.5 mm compared to the weaker grinding of the W sheet-B from 1 to 0.86 mm. For the W bar the elastic modulus is 190 ± 6 GPa. The significantly lower value of E for the W bar might be due to the different microstructure and grain size along the direction of the applied force; also the deformation direction might play a role. The lower value of E for the W bar compared to W sheet is in agreement with its lower value of the ultimate tensile strength found in [16]. The obtained value of E for the W sheet agrees very well with that of pure W produced by mechanical alloying and hot isostatic pressing which was determined employing nanoindentation and found to be 350±40 GPa by Palacios et al. [12].

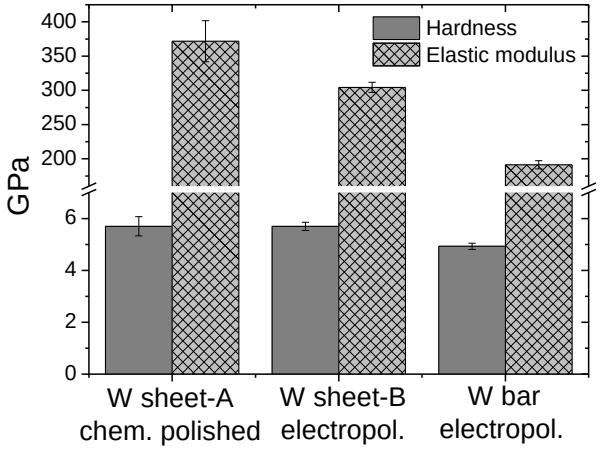

Fig.9. Hardness and elastic modulus for the various W materials for 400 mN maximum load and for holding time and loading/unloading rate of 100 s and 90 nm/min, respectively.

Conclusions

Two tungsten materials, namely a heavily deformed W sheet and a W forged/hammered bar, were investigated employing depth sensing nanoindentation and TEM measurements. The TEM measurements for the W sheet showed a grain size the range 1.5 – 2 μm and an average dislocation density of 3.25×10^{13} m^{-2} (Fig.2). For the W bar the grain size is 0.6 – 1.7 μm and 2.3 – 4 μm, normal to and along the elongation directions, respectively, and the average dislocation density 4.5×10^{12} m^{-2} (Fig.3). The hardness and elastic modulus for the W sheet were investigated as a function of the penetration depth (Fig.5). Hardness is found to follow the Nix-Gao model. The elastic modulus presents a minimum for penetration of 1.5 μm which might be explained by the interaction between the PAZ boundary and the grain/sub-grain interfaces being the dominating mechanism at this depth which is comparable with the sub-grain size. Moreover, the effect of the loading/unloading rate and the holding time at the maximum load was studied and it was found that they do not have any significant influence on the obtained values of H and E. The final surface treatment of the W material, either by electropolishing or chemomechanically polishing, results in the same hardness value of 5.7±0.4 GPa. The elastic modulus of the W sheet is found to be much larger than that of the W bar and the difference is attributed to the different microstructure and grain size along the direction of the applied load.

Acknowledgments

This work was carried out within the EUROfusion Consortium and received funding from the Euratom research and training programme 2014-2018 under grant agreement number No 633053. The views and opinions expressed herein do not necessarily reflect those of the European Commission.

References

[1] Wurster S *et al*. 2013 *J. Nucl. Mater.* **442** S181–S189
[2] Geach G A, Hughes J R 1955 *The Alloys of Rhenium and Molybdenum or with Tungsten and Having Good High Temperature Properties* F. Benesovsky (Ed.), Plansee Proceedings, (Pergamon Pres: London) pp. 245–253
[3] Rieth M, Reiser J, Dafferner B, Baumgärtner S 2012 *Fusion Sci. Technol*. **61** 381–384
[4] Kurishita H, Matsuo S, Arakawa H, Kobayashi S, Nakai K, Takida T, Takebe K, Kawai M 2008 *Mater. Sci. Eng. A* **477** 162–167
[5] Wei Q, Zhang H T, Schuster B E, Ramesh K T, Valiev R Z, Kecskes L J, Dowding R J, Magness L, Cho K 2006 *Acta Mater.* **54** 4079–4089
[6] Riesch J, Buffiere J Y, Höschen T, Di Michiel M, Scheel M, Linsmeier C, You J H 2013 *Acta Mater*. **61** 7060–7071
[7] http://www.euro-fusion.org/
[8] Anthony C Fischer-Cripps 2011 *Nanoindentation* 3rd ed. (New York: Springer)
[9] Pethica J B and Oliver W C 1989 *Mat. Res. Soc. Symp. Proc.* **130** 13-23
[10] Syed Asif S A & Pethica J B 1997 *Phil. Mag. A* **76** 1105-1118
[11] Terentyev D, Bakaeva A, Pardoen T, Favache A, Zhurkin E E 2016 *J. Nucl. Mater.* **476** 1-4
[12] Palacios T, Jiménez A, Muñóz A, Monge M A, Ballesteros C, Pastor J Y 2014 *J. Nucl. Mater.* **454** 455–461
[13] Dubinko A, Terentyev D, Bakaeva A, Pardoen T, Zibrov M, Morgan T W 2017 *Nuclear Instruments and Methods in Physics Research B* **393** 155–159
[14] Dubinko A, Terentyev D, Bakaeva A, Verbeken K, Wirtz M, Hernández-Mayoral M 2017 *Int. Journal of Refractory Metals and Hard Materials* **66** 105–115
[15] Reiser J, Hoffmann J, Jäntsch U, Klimenkov M, Bonk S, Bonnekoh C, Hoffmann A, Mrotzek T, Rieth 2017 *Int. Journal of Refractory Metals and Hard Materials* **64** 261–278
[16] Wirtz M, Uytdenhouwen I, Barabash V, Escourbiac F, Hirai T, Linke J, Loewenhoff Th, Panayotis S and Pintsuk G 2017 *Nucl. Fusion* **57** 066018
[17] Bonk S, Reiser J, Hoffmann J, Hoffmann A 2016 *Int. Journal of Refractory Metals and Hard Materials* **60** 92–98
[18] Manhard A, Matern G and Balden M 2013 *Praktische Metallographie/Practical Metallography* **50** 5-16
[19] Oliver W C and Pharr G M 1992 *J. Mater. Res.* **7** 1564-1583
[20] Oliver W, Pharr G 2004 *J. Mater Res.* **19** 3-20
[21] Hirsch P, Howie A, Nicholson R, Pashley D W, Whelan M J 1997 *Microscopy of Thin Crystals*, (Florida: Krieger Publishing Company Malabar)
[22] Nix W D and Gao H 1998 *J. Mech. Phys. Solids* **46** 411-425
[23] Rester M, Motz C, Pippan R 2009 *J. Mater. Res.* **24** 647−651.
[24] Reiser J, Hoffmann J, Jäntsch U, Klimenkov M, Bonk S, Bonnekoh C, Rieth M, Hoffmann A, Mrotzek T 2016 *Int. Journal of Refractory Metals and Hard Materials* **54** 351–369
[25] Liu G-Y, Ni S, Song M 2015 *Trans. Nonferrous Met. Soc. China* **25** 3240−3246
[26] Durst K, Backes B, Mathias Göken 2005 *Scripta Materialia* **52** 1093–1097
[27] S Graça S, Colaço R, Carvalho P A, Vilar R 2008 *Materials Letters* **62** 3812-3814